Immunotherapy added to antibiotic treatment reduces relapse of disease in a mouse model of tuberculosis

Bas C. Mourik[1], Pieter J.M. Leenen[2], Gerjo J. de Knegt[1], Ruth Huizinga[2], Bram C.J. van der Eerden[3], Jinshan Wang[4], Charles R. Krois[4], Joseph L. Napoli[4], Irma A.J.M Bakker-Woudenberg[1], Jurriaan E.M. de Steenwinkel[1]

[1]*Dept. of Medical Microbiology & Infectious Diseases, Erasmus MC, Rotterdam, the Netherlands*

[2]*Dept. of Immunology, Erasmus MC, Rotterdam, the Netherlands*

[3]*Dept. of Internal Medicine, Erasmus MC, Rotterdam, the Netherlands*

[4]*Department of Nutritional Science and Toxicology, University of California, Berkeley, United States.*

ABSTRACT

Rationale

Immune-modulating drugs that target myeloid-derived suppressor cells or stimulate Natural Killer T-cells have been shown to reduce mycobacterial loads in tuberculosis. We aimed to determine if a combination of these drugs as adjunct immunotherapy to conventional antibiotic treatment could also increase therapeutic efficacy against tuberculosis.

Methods

In our model of pulmonary tuberculosis in mice, we applied treatment with isoniazid, rifampicin and pyrazinamide for 13 weeks alone or combined with immunotherapy consisting of all-trans-retinoic acid, 1,25(OH)2-vitamin D3 and α-galactosylceramide. Outcome parameters were mycobacterial load during treatment (therapeutic activity) and 13 weeks after termination of treatment (therapeutic efficacy). Moreover, cellular changes were analyzed using flow cytometry and cytokine expression was assessed at mRNA and protein level.

Results

Addition of immunotherapy was associated with lower mycobacterial loads after 5 weeks of treatment and significantly reduced relapse of disease after a shortened 13-weeks treatment course compared to antibiotic treatment alone. This was accompanied by reduced accumulation of immature myeloid cells in the lungs at the end of treatment and increased TNF-α protein levels throughout the treatment period.

Conclusion

We demonstrate in a mouse model of pulmonary tuberculosis that immunotherapy consisting of three clinically approved drugs can improve the therapeutic efficacy of standard antibiotic treatment.

Published in the American Journal of Respiratory Cell and Molecular Biology
2017 Feb;56(2):233-241. doi: 10.1165/rcmb.2016-0185OC.

INTRODUCTION

Annually, an estimated 9 million people worldwide develop active tuberculosis (TB) and rates of multidrug-resistant and extensively drug-resistant TB continue to rise (1). In the search for improved and shortened treatment regimens to counter the TB pandemic, immunotherapy as an adjunct to antibiotic treatment is gaining interest (2).

Several strategies in this regard are currently being explored, including the use of immunoglobulins, statins and metformin (3). Another option that may contribute to anti-TB treatment is targeted inhibition of myeloid-derived suppressor cells (MDSC) (4). MDSC are immature myeloid cells that accumulate during pathological inflammatory conditions and have the functional ability to suppress T-cell proliferation and to inhibit IFN-g production (5). In mice, MDSC are broadly defined as $CD11b^+$ $Gr1^+$ cells. However, as they phenotypically resemble their non-suppressive counterparts developing under steady state conditions, MDSC can only be identified unequivocally based on functional testing (5, 6).

The detrimental function of MDSC in TB has been demonstrated in both mouse models (4, 7-9) and in patient populations (10, 11). Moreover, in mouse TB, MDSC that infiltrated the lungs phagocytosed Mycobacterium tuberculosis, thereby creating a potential niche for pathogen survival.

The inhibitory function of MDSC can be targeted with all-trans-retinoic acid (ATRA) (12). This vitamin A-derivative was shown to induce maturation and thereby functional depletion of MDSC (13). In experimental TB in mice and rats, ATRA therapy reduced the number of MDSC (4), lowered mycobacterial loads in the lungs in vivo (4, 14), and stimulated antimicrobial activity against *Mycobacterium tuberculosis* (Mtb) in vitro (15, 16). The maturation effect of ATRA on MDSC could be enhanced by adding $1,25(OH)_2$-vitamin D3 (DiOH-VD3) (17), which in itself also stimulated antimicrobial activity against Mtb that is mechanistically distinct from ATRA's mode of action (15).

Lastly, ATRA increased the expression of CD1d on antigen presenting cells, which is required for activation of Natural Killer T-cells (NKT cells) (18). CD1d-dependent activation of NKT cells with the CD1d ligand α-GalactosylCeramide (α-GalCer) reduced mycobacterial loads and improved survival in mice with TB (19). Since the combination of ATRA and α-GalCer has been found to convert MDSC into immunogenic antigen-presenting cells (20), we added α-GalCer to our treatment so as to combine differentiation therapy with activation of CD1d-restricted NKT cells.

The contributions ATRA and α-GalCer to therapy in TB are limited to therapeutic activity studies, determining reduction in mycobacterial load (4, 19). However, therapeutic activity was shown to be a poor predictor of therapeutic efficacy in TB, which can be determined by survival or relapse studies (21, 22). Therefore, to test the above-mentioned therapeutics in a setting more similar to clinical conditions, we determined if a combination of ATRA, DiOH-VD3 and α-GalCer could increase the therapeutic efficacy of antibiotic treatment, allowing shortening of TB treatment duration from 26 weeks to 13 weeks. We performed these studies in our model of pulmonary TB in mice, optimized to simulate the full course of TB treatment in humans according to WHO recommendations (23, 24).

MATERIALS AND METHODS

Mice, bacteria and infection

Female specific pathogen-free BALB/c mice aged 10-11 weeks and weighing 22-24 grams (Charles River, Les Oncins, FR) were infected with the H37Rv Mtb strain (ATCC 27294) by intra-tracheal instillation of 1.0-2.9x10^5 mycobacteria under general anesthesia as described previously (25). Inoculum sizes were confirmed by plating. All protocols were approved by the institutional animal ethics committee and adhered to the rules laid down in the Dutch Animal Experimentation Act and the EU Animal Directive 201/63/EU, DEC number 117-12-07, EMC-number 2737.

Treatment regimens

Choice of antibiotic drugs and dosage schedules were in accordance with the WHO guidelines for treatment of TB as described previously (25). In short, treatment started 4 weeks post infection (p.i.) and consisted of isoniazid (H, 25 mg/kg), rifampicin (R, 10 mg/kg) and pyrazinamide (Z, 150 mg/kg) administered subcutaneously in the neck once daily for five days a week (Mo-Fri). The DiOH-VD3 (Sigma Chemical Co, St. Louis, MO, USA) was frozen as 10% stock solution in 100% ethanol and was diluted in sterile 0.9% NaCl prior to administration. DiOH-VD3 was injected intraperitoneally in a volume of 500 µL containing 0.05 µg DiOH-VD3 three days per week (Mo-We-Fri). Dose and route of administration resulted in human pharmacokinetic equivalent dosage (26). α-GalCer (Tebu-bio, Le Perray-en-Yvelines, France) was dissolved as described previously (27) and was injected intraperitoneally at 500 µg/kg in a total volume of 300 µL at day 1 of treatment and subsequently once every 30 days conform to treatment of TB in an earlier study (19). ATRA was administered using slow release drug pellets (4 or 10 mg, 90-days sustained release pellets; Innovative Research of America, Sarasota, FL, USA). Pellets were implanted subcutaneously in the flank under general anesthesia.

Real-time quantitative PCR

RNA from mouse lung homogenate was purified and processed as described previously (28). Sequences for primers and reference numbers for probes (Universal Probe Library; Roche Applied Science) are listed in **Table E1** in the supplementary data. RNA levels were calculated relative to RNA levels of household gene *Gapdh*.

Flow cytometry

The flow cytometry protocol is explained in detail in the online data supplement. To eliminate live mycobacteria prior to flow cytometry analysis, cell suspensions were fixed for 30 min in fix/perm solution (Ebioscience, Vienna, AT). Cells were stained with different mAb mixes as described in **Table E2** in the supplementary data and measured on a FACS Canto II flow cytometer (BD Biosciences, Breda, NL).

Data analysis and statistics

Flow cytometry data were analyzed using Flowjo 7.6.5. Analyses were done and graphs were made using PRISM Graphpad 6. All data are expressed as mean ± SEM. Student's t-test, followed by Bonferroni correction where applicable, was used to calculate significance unless stated otherwise. P-values less than 0.05 were considered statistically significant.

Supplemental data

Tissue handling, mycobacterial load determination, ATRA and Ca^{2+} serum level quantification and lung supernatant cytokine level quantification are described in detail in the online data supplement.

RESULTS

TB leads to increased ATRA serum concentration during treatment

Since ATRA has a narrow therapeutic window (29), we first performed dose finding in uninfected mice with ATRA as single adjunct to treatment with isoniazid, rifampicin and pyrazinamide (HRZ) before starting combination therapy. Based on loss of bodyweight and supported by animal wellbeing scores, ATRA therapy in a dose of 5 mg/kg/day (10 mg pellets) was well tolerated and addition of HRZ did not influence ATRA serum concentrations in uninfected mice (**Fig. 1A**). However, in Mtb-infected mice we found ATRA serum concentrations 2-3-fold higher compared to uninfected ATRA-treated mice, which was associated with excessive weight loss (**Fig. 1B**). A lower ATRA dose of 2 mg/kg/day (4 mg pellets) was well tolerated by Mtb-infected mice and was still associated with a 10-fold increase of physiological ATRA serum concentrations to 11.9 ± 0.2 pmol/

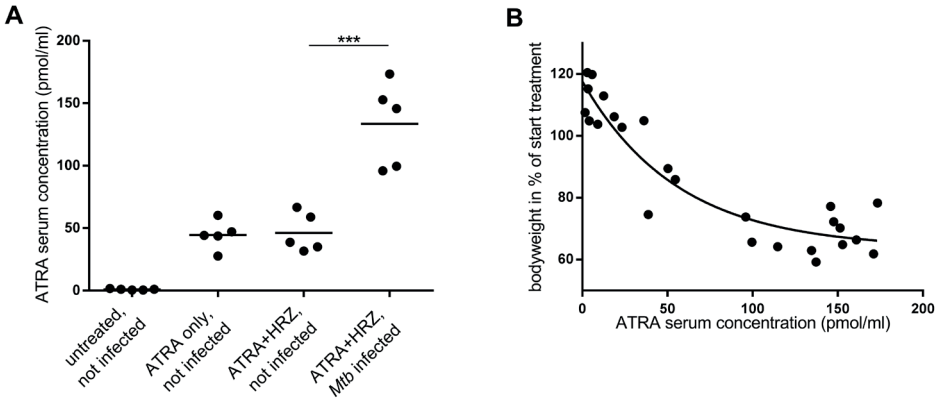

Figure 1. ATRA serum concentrations increase upon ATRA-treatment during Mtb infection and are associated with excessive body weight loss.

A) After 25 days of treatment, ATRA serum concentrations were measured in uninfected and Mtb-infected mice treated with ATRA, eventually supplemented with antibiotics (HRZ). ATRA was applied as 10 mg, 90-days release pellets. ATRA serum concentrations were not affected by addition of HRZ, but were significantly increased when treatment was started 4 weeks after infection with Mtb (***$p < 0.001$). **B)** Pooled data from different experiments for ATRA serum concentrations versus body weight loss in Mtb-infected mice after 21 to 35 days of treatment with ATRA+HRZ using 10 mg 90-days sustained release pellets. ATRA serum concentration was strongly correlated with body weight loss (R^2: 0.88).

ml (**Fig. E1** in the supplementary data). Therefore, ATRA was applied in this lower dose in our experiments.

Adjunct immunotherapy is well tolerated and marginally increases therapeutic activity

Next, we determined the therapeutic activity of immunotherapy consisting of ATRA, DiOH-VD3 and α-GalCer (ADG) adjunct to antibiotic treatment with isoniazid, rifampicin and pyrazinamide (HRZ). To this aim, we used the BALB/c mouse model of Mtb infection. In this model, mice reach the peak of infection at 4 weeks post infection with Mtb loads of 10^6-10^8 in the lungs and of 10^4-10^6 in spleen and liver. Mycobacterial loads subsequently stabilize and untreated mice become moribund between 22 and 38 weeks after infection (25).

At the peak of infection treatment was initiated with HRZ or HRZ+ADG for a period of 5 weeks. After termination of treatment, HRZ+ADG-treated mice had three-fold lower mycobacterial loads in the spleen ($p<0.05$) and showed a trend towards lower mycobacterial loads in the lungs (2.7-fold lower, $p=0.08$) compared to HRZ-treated mice (**Fig. 2A**).

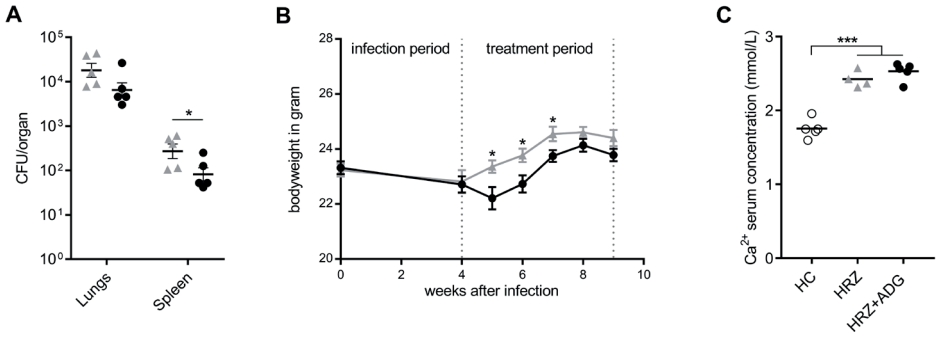

Figure 2. Addition of ADG to HRZ therapy is well tolerated and enhances mycobacterial killing during active disease.

A) Mycobacterial loads in the lungs and spleen after 5 weeks of treatment (9 weeks p.i.) with HRZ (grey triangles) or HRZ+ADG (black dots), n=5 mice per group. **B)** Bodyweight in grams during infection and treatment. **C)** Serum concentrations of Ca^{2+} in Mtb-infected mice treated with HRZ or HRZ+ADG after 5 weeks of treatment (9 weeks p.i.) compared to healthy controls. In untreated mice mycobacterial loads in the lungs and spleen at 9 weeks p.i. are 10^7 and 10^5 respectively (published earlier in (25).Data are derived from a single experiment and shown as mean ± SEM. Mycobacterial loads in antibiotic-treated mice are in agreement with previous historic controls (25). *** $p < 0.001$, **$p < 0.01$, *$p < 0.05$. HC=healthy control, HRZ= isoniazid, rifampicin and pyrazinamide, ADG= ATRA, DiOH-VD3 and α-GalCer.

Regarding tolerability, HRZ+ADG-treated mice weighing >20 grams at start of treatment transiently lost weight compared to HRZ-treated mice (**Fig. 2B**). However, mice weighing ≤20 gram 4 weeks p.i. showed excessive weight loss in the first week of treatment and had to be euthanized as they had reached humane endpoints. Therefore, mice weighing ≤20 gram at start of treatment were excluded in both treatment groups (2 mice from each group).

Treatment with ATRA- or DiOH-VD3, but also TB itself, can all cause hypercalcaemia. Therefore, serum Ca^{2+} was determined at end of treatment. The Ca^{2+} levels in both HRZ or HRZ+ADG treatment groups were significantly higher than in uninfected mice, but did not differ between the two treatment groups (**Fig. 2C**).

Adjunct immunotherapy reduces relapse of disease

In order to determine the effect of ADG adjunct therapy on therapeutic efficacy, our next step was to measure relapse of TB. In previous experiments in our mouse TB model, mycobacterial loads in infected tissues became undetectable after 13 weeks of HRZ treatment (25). However, when treatment was terminated at this point instead of completing the WHO-recommended 26 weeks period, relapse of disease still occurred leading to mycobacterial loads of circa 10^3 CFU in the lungs (25). To determine the effect of ADG therapy against these persistent Mtb populations responsible for relapse of

disease, we treated Mtb-infected mice for 13 weeks with HRZ or HRZ+ADG. Next, at 13 weeks after termination of treatment, i.e. at 30 weeks p.i., we measured mycobacterial loads in lungs and spleen (**Fig. 3A**). We validated our data with regard to infection kinetics by comparing it to earlier findings in this model. In line with previous findings, mice from both groups had low or undetectable mycobacterial loads in the lungs after 13 weeks of treatment (25). At 30 weeks p.i., relapse of disease with mycobacterial loads of 10^3 in the lungs was observed in only 1 out of 8 HRZ+ADG-treated mice versus 6 out of 8 HRZ-treated mice ($p < 0.05$). In addition, one HRZ-treated mouse had Mtb in the spleen ($10^{2.4}$ CFU, data not shown) versus none of the HRZ+ADG-treated mice. In 3 mice from the HRZ+ADG-treated group, minimal mycobacterial loads were still detectable at 30 weeks p.i., but none exceeded those found 17 weeks p.i. (**Fig. 3B**). Interestingly, serum Ca^{2+} levels in the HRZ+ADG-treated group were significantly lower than in HRZ-treated mice at the end of the post-treatment period, but still higher than in healthy control mice (**Fig. 3C**).

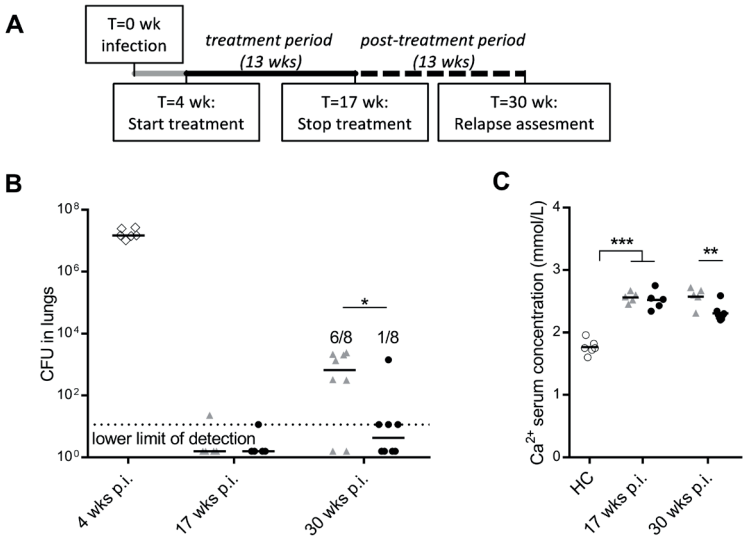

Figure 3. Addition of ADG to HRZ therapy significantly reduces relapse of disease.
A) Outline of the experimental design. **B)** Mice were treated with HRZ (grey triangles) or HRZ+ADG (black dots) starting 4 weeks p.i. (open diamonds). Lung mycobacterial loads were determined by plating. At 17 weeks p.i. both treatment groups still had 1 mouse with a detectable mycobacterial load in the lungs (HRZ only: $10^{1.4}$ HRZ+ADG: $10^{1.1}$). At 30 weeks p.i. 3 mice from the HRZ+ADG treated group had detectable mycobacterial loads (all: $10^{1.1}$). Fisher's exact test was used to calculate significance between relapse vs. no relapse at 30 weeks p.i. Of note: in untreated mice mycobacterial loads in the lungs remain constant between 10^6-10^8 from week 4 up to week 30 (25) **C)** Serum concentrations of Ca^{2+} at each time point as shown in **B** in both treatment groups compared to healthy controls (open circles). Data are derived from a single experiment and shown as mean ± SEM, n=5 mice per group at 4 and 17 wk p.i., n=8 mice per group at 30 wk p.i. ***$p < 0.001$, **$p < 0.01$, *$p < 0.05$, HRZ= isoniazid, rifampicin and pyrazinamide, ADG= ATRA, DiOH-VD3 and α-GalCer.

To verify adequate release of ATRA throughout the treatment period the remaining amount of ATRA in the pellets of sacrificed mice 17 weeks p.i. was measured. These still contained 100 ± 18 µg of ATRA (2.5% of original content). Serum concentrations of ATRA at 17 weeks p.i. were elevated compared to concentrations earlier found in healthy control mice, but were no longer elevated at 30 weeks p.i. (**Fig. E1** in the supplementary data). The small amounts of ATRA found in the pellets at 17 weeks p.i. as well as serum levels over time suggest an adequate release of the 4 mg ATRA content over the treatment period.

Addition of ADG to HRZ therapy modulates the cellular immune response in TB.

To assess the immune-modulating effects associated with ADG we measured the composition of immune cell populations in the lungs during infection and treatment. Since the components of ADG primarily target myelomonocytic cells, we focused on the myeloid populations in the lungs, identified primarily by high level CD11b expression.

First we identified the different $CD11b^+$ cell populations in the lungs during steady state and infection (**Fig. 4A**). These consisted of alveolar macrophages, inflammatory macrophages/dendritic cells, PMN-like cells, monocyte (Mo)-like cells and eosinophils (see: **Table 1)**. A small $CD11b^+CD68^-Ly6G^-$ population, earlier shown to consist mainly of NK-cells and CD11b+ T-cells, was also identified (30). For the non-myeloid cell populations gating strategies can be found in **Fig. E2** in the supplementary data.

Table 1. Identified cell populations in the lung

Cell type	Identification
CD4+ T-cells	$CD3^+/CD4^+$
T-reg cells	$CD3^+/CD4^+/FoxP3^+/CD25^+$
CD8+ T-cells	$CD3^+/CD8^+$
B-cells	$CD45R^+/MHC\text{-}II^+/Ly6C^-$
Alv. Mϕ	$CD11b^{int}/Siglec\text{-}F^+/CD11c^{high}$
iM/DC	$CD11b^+/MHC\text{-}II^+/CD11c^{int}/Ly6C^{int}$
Mo-like cells	$CD11b^+/MHC\text{-}II^-/CD11c^-/Ly6C^{high}$
PMN-like cells	$CD11b^+/Ly6G^+/Ly6C^{int}$
Eosinophils	$CD11b^+/ Siglec\text{-}F^+$

In the acute phase of infection until the start of treatment at week 4 p.i. almost all myeloid and non-myeloid cell populations increased in the lungs of infected mice (**Fig. 4B**). Focusing on immature myelomonocytic cells as potential MDSC we found a strongly diminished expression of Ly6G in our PMN-like population (pop. IV) at 4 weeks p.i. compared to healthy controls (**Fig. 4C**), similar to earlier described MDSC identified

as CD11b^{+} Ly6G^{dim} cells (7, 8). Upon treatment, Ly6G expression on the PMN-like cells increased in both groups, but more rapidly in the HRZ+ADG-treated group than in the group receiving only HRZ.

Upon 5 weeks of treatment (9 weeks p.i.) all myeloid cell populations rapidly decreased to below their steady state, with the exception of PMN-like cells (**Fig. 5A**). The latter returned to steady state level in the HRZ+ADG-treated group, while being markedly reduced in the HRZ-treated group. At the end of treatment (17 weeks p.i.), PMN-like cell

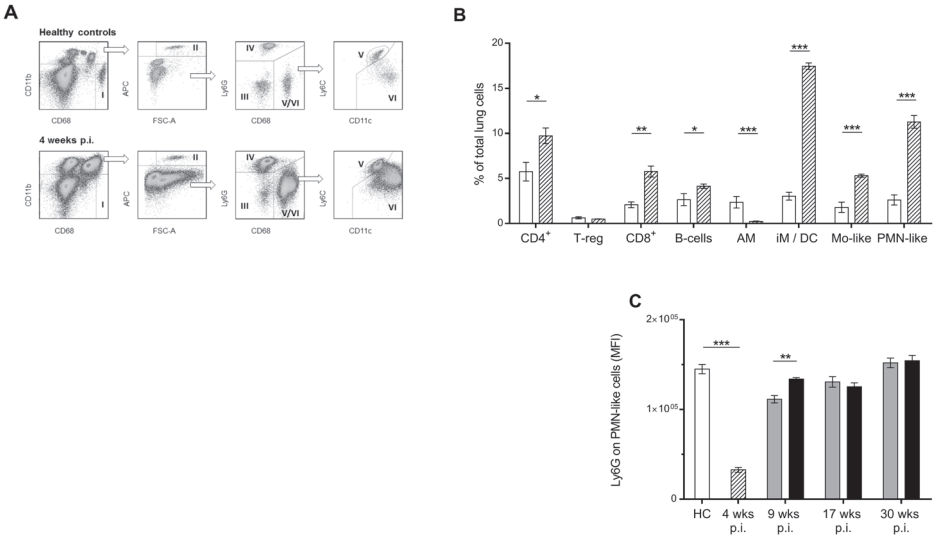

Figure 4. Addition of ADG to HRZ therapy is associated with faster recovery of Ly6G expression on PMN-like cells

A) Separation of the different CD11b+ cell populations in whole lung single cell suspension in steady state and in Mtb-infected mice at 4 weeks p.i. We first separated the AM (I) based on their reduced expression of CD11b and high expression of macrosialin (CD68), followed by eosinophils (II) based on their high auto fluorescence in the APC channel (CD117), but also based on their expression of Siglec-F (see **Fig. E2B** in the supplementary data). Next, based on their lack of expression of both Ly6G and CD68, a population known earlier to exist of T-cells and NK-cells (III) was identified. The PMN-like cells (IV) were separated based on Ly6G expression and lack of CD68 expression. Finally the CD68+ population was divided into Mo-like cells (V) and iM/DC (VI) based on their differential expression of Ly6C and CD11c. **B)** Quantitative comparison of the different cell populations as shown in **Table 1** in whole lung single cell suspension between steady state (HC, open bars) and 4 weeks p.i. (striped bars) shows a sharp increase of all inflammatory myeloid cells, a reduction in AM and an increase of mainly CD8+ cells and B-cells in the lymphoid cell compartment. **C)** Ly6G expression on PMN-like cells during infection and under treatment with HRZ (grey bars) or HRZ+ADG (Black bars). Cell populations are shown as mean ± SEM, ***p < 0.001, **p < 0.01, *p < 0.05, n=5 per group at 9 weeks p.i. and 17 weeks p.i., n=8 per group 30 weeks p.i. Data are from the same mice used for experiments shown in **Fig. 2-3**. HC= healthy controls, AM=alveolar macrophages, Mo= monocytic, PMN= polymorphonuclear, iM/DC= inflammatory macrophage/dendritic cells, HRZ= isoniazid, rifampicin & pyrazinamide, ADG= ATRA, DiOH-D3 and α-GalCer.

numbers were similar in both groups. However, at this point the iM/DC and their precursor population of Mo-like cells were reduced in the HRZ+ADG-treated group (**Fig. 5B**). At the end of the post-treatment and potential relapse period (30 weeks p.i.) there were no differences in myeloid cell populations between the two treatment groups and healthy control mice (**Fig. 5C**).

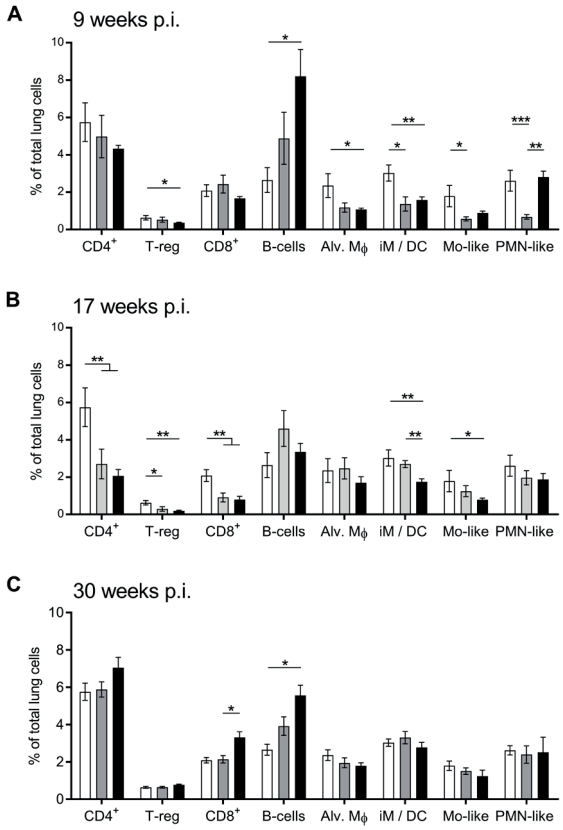

Figure 5. Addition of ADG to HRZ therapy is associated with fewer iM/DC at end of treatment and more CD8$^+$ T-cells at 30 weeks p.i.

A) Quantitative comparison of the different cell populations as shown in **Table 1** in whole lung single cell suspension between the two treatment groups at 9 weeks p.i. The PMN-like cells in the HRZ-treated group (grey bars) are markedly suppressed compared to HRZ+ADG-treated mice (black bars) and uninfected mice (open bars). **B)** At 17 weeks p.i. iM/DC are reduced in HRZ+ADG-treated mice compared to HRZ-treated mice **C)** At 30 weeks p.i. CD8$^+$ cells are increased in the HRZ+ADG-treated mice compared to HRZ-treated mice. Cell populations are shown as mean ± SEM, ***p < 0.001, **p < 0.01, *p < 0.05 after Bonferroni correction, n=5 per group at 9 weeks p.i. and 17 weeks p.i., n=8 per group at 30 weeks p.i. Data are from the same mice used for experiments shown in **Fig. 2-3**. HC= healthy controls, AM=alveolar macrophages, Mo= monocytic, PMN= polymorphonuclear, iM/DC= inflammatory macrophage/dendritic cells, HRZ= isoniazid, rifampicin & pyrazinamide, ADG= ATRA, DiOH-D3 and α-GalCer.

Concerning non-myeloid cells there were no significant differences between the two treatment groups during treatment at 9 weeks p.i. (**Fig. 5A**). At the end of treatment T-cells were significantly suppressed in both groups compared to steady state (**Fig. 5B**). At 30 weeks p.i. the HRZ+ADG-treated group had significantly higher percentages of $CD8^+$ T-cells compared to the HRZ-treated group (**Fig. 5C**).

Addition of ADG to HRZ therapy increases TNF-α protein levels.

To identify the cytokine response associated with ADG adjunct therapy we measured cytokine expression at mRNA and protein level during infection and treatment. At the peak of infection, 4 weeks p.i., mRNA expression of IFN-g, IL-6 and IL-17a was increased, but expression of TNF-α was reduced compared to steady state (**Fig. 6A**). Protein levels

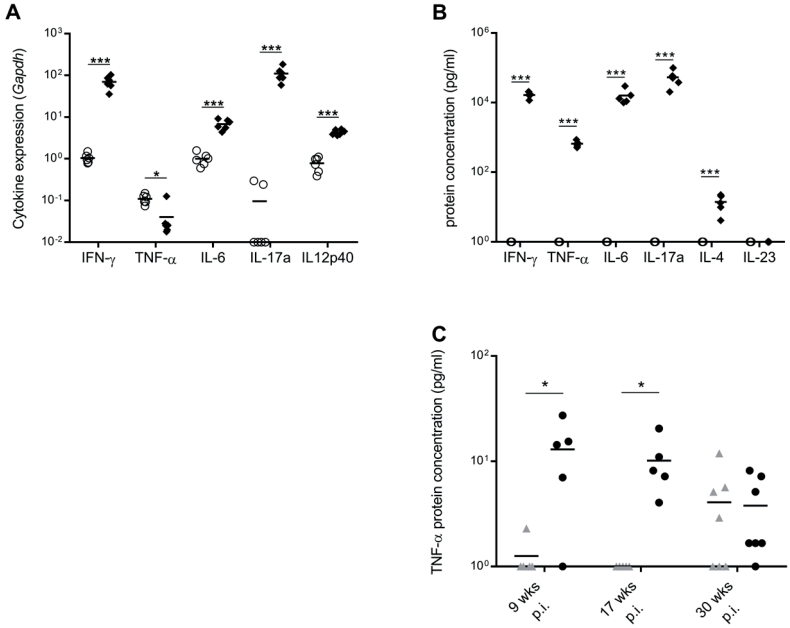

Figure 6. Addition of ADG to HRZ treatment is associated with increased TNF-α protein levels during treatment

A) Gene expression analysis of key cytokines in whole lung homogenate normalized to the expression of *Gapdh*. 4 weeks p.i. (black diamonds) compared to steady state (open circles). **B)** Cytokine protein concentration analysis in whole lung homogenate supernatant 4 weeks p.i., **C)** TNF-α protein concentrations after 5 weeks of treatment (9 wks p.i.), 13 weeks of treatment (17 wks p.i.) and 13 weeks after termination of treatment (30 wks p.i.) with HRZ (grey triangles) or HRZ+ADG (black dots). Significance for TNF-α was corrected for 1 outlier at 9 wks p.i. (with outlier included: p= 0.03, NS after Bonferroni correction, with outlier excluded: p=0.004, * after Bonferroni correction) *** $p < 0.001$, **$p < 0.01$, *$p < 0.05$ after Bonferroni correction, n=5 per group at 9 weeks p.i. and 17 weeks p.i., n=8 per group 30 weeks p.i. Data are from the same mice used for experiments shown in **Fig. 2-3**.

correlated with mRNA expression for IFN-g, IL-6 and IL-17a**,** but TNF-α protein levels were substantially increased (**Fig. 6B**) despite reduced mRNA expression.

During and after treatment, TNF-α mRNA expression did not differ significantly between both groups (**Fig. E3** in the supplementary data). However, protein levels of TNF-α in HRZ+ADG-treated mice were significantly increased compared to HRZ-treated mice at 9 weeks p.i. and 17 weeks p.i. (**Fig. 6C**).

Messenger RNA (mRNA) expression of IFN-g, IL-17a and IL-6 remained increased in both treatment groups at 9, 17 and 30 weeks p.i., but these increases were not observed at protein level and no significant differences were found between the two treatment groups (**Fig. E3-4** in the supplementary data). IL-4 protein levels were increased 4 weeks p.i. (**Fig 6B**) and persisted at this level throughout the examination period (**Fig E4** in the supplementary data). Lastly, IL-10 mRNA expression and IL-10 protein levels were both below our limit of detection (data not shown).

DISCUSSION

We determined if adjunct immunotherapy with drugs known to reduce mycobacterial loads in the lungs could increase long term therapeutic efficacy of the WHO-recommended antibiotic treatment. In our mouse TB model we have found that a combination of ATRA, DiOH-D3 and α-GalCer was tolerated at the given dosage, increased antibiotic-mediated reduction of mycobacterial loads in infected organs after 5 weeks of treatment, reduced the levels of immature myeloid cells in the lungs at the end of treatment, and was associated with 10-fold increased levels of TNF-α protein in the lungs throughout the treatment period. Even more, addition of ADG significantly reduced relapse of disease and was associated with nearly twice the levels of $CD8^+$ T-cells, compared to HRZ alone 13 weeks after termination of treatment.

To our knowledge, this is the first study in which serum concentrations of ATRA were determined when added as a supplement to therapy in TB and we found an important association between fulminant TB and pathologically elevated ATRA serum concentrations. This can probably be ascribed to altered ATRA pharmacokinetics during infection. In our in vivo TB model, Mtb have already spread from the lungs to the liver 4 weeks p.i. (23). Local inflammation and bacterial infection are known to impair CYP450-mediated drug metabolism in the liver, resulting in increased ATRA levels (38). The use of ATRA as a single therapeutic agent for TB has been tested earlier (4, 14). In those two studies ATRA

treatment was started earlier in the course of infection, i.e. before bacterial dissemination to the liver occurred, and ATRA-associated weight loss was not reported.

Other studies have demonstrated that functionally suppressive MDSC accumulate during acute TB in the lungs of mouse strains that are either less or more susceptible than the currently used BALB/c mice (4, 7, 9) and that these MDSC could be targeted successfully with ATRA (4). These findings inspired us to evaluate the therapeutic efficacy of ATRA in TB in combination with two synergistic immune-modulating drugs (17, 20). Both ATRA and α-Galcer as single drug therapy earlier lowered mycobacterial loads in the lungs with a range between log 0.5 and log 2 after different treatment regimens and durations (4, 14, 19). For α-GalCer it has been shown that its effect is CD1d-dependent, but ATRA also has a direct bacteriostatic effect that could contribute to the reduced mycobacterial loads observed in both the reported (4) and the present study. However, this direct bacteriostatic effect was only demonstrated *in vitro* with ATRA concentrations well above serum concentrations found in our study (16). For α-GalCer it has been shown that reductions in CFU persist when isoniazid is concomitantly administered (19). We demonstrate that when tested as adjuvant to the full HRZ regimen, a combination of ATRA, α-GalCer and DiOH-VD3 marginally improves therapeutic activity. We do not consider it likely that this could be of major clinical significance. Elaborating on this, clinical studies indicate that anti-mycobacterial activity, as measured in early bactericidal activity assays (EBA), is a poor predictor of therapeutic efficacy (21, 22).

With regard to therapeutic efficacy, it has been demonstrated previously that α-GalCer prolongs survival of Mtb-infected mice (19). However no data are available in the context of the most clinically relevant scenario, which is concomitant administration adjunct to the current antibiotic anti-TB regimen. Using the BALB/c mouse model as a well-recognized experimental approach for efficacy studies (31, 32), our relapse data demonstrate that adjunct ADG therapy improved the therapeutic efficacy of HRZ treatment, but was not sufficient to eliminate all Mtb during a 13 week treatment course. This is supported by the observation that at 30 weeks p.i., Ca^{2+} levels, which correlate with disease activity in TB (33), were significantly higher in the HRZ-treated group, but also remained elevated in the HRZ+ADG-treated group compared to healthy controls. In addition, both treatment groups showed elevated IFN-g mRNA expression and increased IL-4 and TNF-α protein levels compared to steady state 30 weeks p.i. Lastly, mycobacteria were still detectable in the lungs of some mice from the HRZ+ADG group that did not relapse. Taken together, these observations suggest that HRZ+ADG-treatment was not able to clear infection completely in this TB model but did significantly improve containment of infection compared to treatment with antibiotics only.

Based on published results of single-drug experiments and synergy reported between the individual components (17, 20), we chose ADG to potentiate host immunity, in particular targeting MDSC activity. However, we did not prove the latter to be the main mechanism of action by performing functional MDSC testing. Hence, we only describe correlations between treatment modality and changes in immune parameters. At the peak of infection the $CD11b^{+}Ly6G^{dim}$ PMN-like cells from our model phenotypically resembled the $CD11b^{+}Ly6G^{dim}$ MDSC population found earlier (7). However, during treatment these immature cells with reduced Ly6G expression could no longer be found. Given the sharp reduction of PMN-like cells in the lungs during antibiotic treatment and their rapid change in phenotype towards more mature, conventional PMN, we consider it likely that functional MDSC activity by the PMN-like cell population is concomitantly reduced. In line with this, increased numbers of MDSC have been found in patients after recent TB infection and active disease, but successful anti-TB treatment significantly reduced MDSC numbers and coincided with increased MDSC maturation (10). On the other hand, overall adaptive immune cells are increased at 30 weeks p.i. in mice from the HRZ+ADG-treated group with significantly more $CD8^{+}$ cells in the lungs, but without differences in the myeloid compartment or cytokine profile between the two treatment groups.. This suggests reduced functional MDSC-activity in the HRZ+ADG-treated group, which is supported by studies showing that MDSC inhibit $CD8^{+}$ T-cells primarily in a contact-dependent way and reduce $CD8^{+}$ T-cell infiltration (5, 34). However, in the context of the current study this remains speculative.

Apart from the potential role of MDSC, we observed increased levels of TNF-α protein in the HRZ+ADG-treated group during treatment, which could have contributed to the improved therapeutic efficacy. TNF-α is a critical immune mediator in TB and holds a central protective position in the balance between an adequate anti-TB response, excessive inflammation-induced pathology, and reactivation of latent disease (35).. We observed discrepancies between TNF-α mRNA expression and protein levels that were not found for other cytokines tested. This is likely due to post-transcriptional regulation to which TNF-α is exceptionally prone (36), as is also observed in TB (37). If enhancing TNF-α production is indeed a key factor mediated by ADG adjunct therapy, treatment initiation should be timed carefully, since increased TNF-α levels during the active phase of disease might also explain the initial bodyweight loss in the HRZ+ADG-treated group in the first 3 weeks of treatment. In support of this ambiguous role of TNF-α, a recent in vivo study showed increased therapeutic efficacy of TNF-α inhibition (38), further demonstrating the complexity of the interplay between TB and immune modulation strategies. These data together suggest that it might be more beneficial to treat TB initially with antibiotics only and add ADG later in order to increase sterilizing immune activity.

In conclusion, we have shown that a combination of three clinically approved drugs as an adjunct to current HRZ treatment can modulate the immune response and improve therapeutic efficacy in TB. This adds to the possibility of adjunct immunotherapy as viable treatment modality in TB. In the current study we demonstrate a proof of principle with clinical potential. However, based on the experimental design and data obtained, the therapeutic mechanism of ADG on a cellular and molecular level and the role of MDSC were not identified unequivocally, which should be addressed in forthcoming studies.

ACKNOWLEDGEMENTS

The authors thank S. van den Berg, M.T. ten Kate, M.A.W. Smits, A. van Oudenaren and M. Schreuders-Koedam for their technical support, and J. Hagoort and D. Drevets for their critical reading of the manuscript.

REFERENCES

1. WHO Global tuberculosis report 2014.
2. Zumla A, Nahid P, Cole ST. Advances in the development of new tuberculosis drugs and treatment regimens. *Nat Rev Drug Discov* 2013;12(5):388-404.
3. Wallis RS, Hafner R. Advancing host-directed therapy for tuberculosis. *Nat Rev Immunol* 2015;15(4):255-263.
4. Knaul JK, Jorg S, Oberbeck-Mueller D, Heinemann E, Scheuermann L, Brinkmann V, Mollenkopf HJ, Yeremeev V, Kaufmann SH, Dorhoi A. Lung-residing myeloid-derived suppressors display dual functionality in murine pulmonary tuberculosis. *Am J Respir Crit Care Med* 2014;190(9):1053-1066.
5. Gabrilovich DI, Nagaraj S. Myeloid-derived suppressor cells as regulators of the immune system. *Nat Rev Immunol* 2009;9(3):162-174.
6. Ribechini E, Leenen PJ, Lutz MB. Gr-1 antibody induces STAT signaling, macrophage marker expression and abrogation of myeloid-derived suppressor cell activity in BM cells. *Eur J Immunol* 2009;39(12):3538-3551.
7. Tsiganov EN, Verbina EM, Radaeva TV, Sosunov VV, Kosmiadi GA, Nikitina IY, Lyadova IV. Gr-1^{dim}cd11b^{+} immature myeloid-derived suppressor cells but not neutrophils are markers of lethal tuberculosis infection in mice. *J Immunol* 2014;192(10):4718-4727.
8. Lyadova IV, Tsiganov EN, Kapina MA, Shepelkova GS, Sosunov VV, Radaeva TV, Majorov KB, Shmitova NS, van den Ham HJ, Ganusov VV, et al. In mice, tuberculosis progression is associated with intensive inflammatory response and the accumulation of Gr-1^{+} cells in the lungs. *PLoS One* 2010;5(5):e10469.
9. Obregon-Henao A, Henao-Tamayo M, Orme IM, Ordway DJ. Gr1^{int}cd11b^{+} myeloid-derived suppressor cells in *Mycobacterium tuberculosis* infection. *PLoS One* 2013;8(11):e80669.
10. du Plessis N, Loebenberg L, Kriel M, von Groote-Bidlingmaier F, Ribechini E, Loxton AG, van Helden PD, Lutz MB, Walzl G. Increased frequency of myeloid-derived suppressor cells during active tuberculosis and after recent *Mycobacterium tuberculosis* infection suppresses T-cell function. *Am J Respir Crit Care Med* 2013;188(6):724-732.
11. Yang B, Wang X, Jiang J, Zhai F, Cheng X. Identification of CD244-expressing myeloid-derived suppressor cells in patients with active tuberculosis. *Immunol Lett* 2014;158(1-2):66-72.
12. Kusmartsev S, Cheng F, Yu B, Nefedova Y, Sotomayor E, Lush R, Gabrilovich D. All-trans-retinoic acid eliminates immature myeloid cells from tumor-bearing mice and improves the effect of vaccination. *Cancer Res* 2003;63(15):4441-4449.
13. Mora JR, Iwata M, von Andrian UH. Vitamin effects on the immune system: Vitamins A and D take centre stage. *Nat Rev Immunol* 2008;8(9):685-698.
14. Yamada H, Mizuno S, Ross AC, Sugawara I. Retinoic acid therapy attenuates the severity of tuberculosis while altering lymphocyte and macrophage numbers and cytokine expression in rats infected with *Mycobacterium tuberculosis*. *J Nutr* 2007;137(12):2696-2700.
15. Wheelwright M, Kim EW, Inkeles MS, De Leon A, Pellegrini M, Krutzik SR, Liu PT. All-trans retinoic acid-triggered antimicrobial activity against *Mycobacterium tuberculosis* is dependent on NPC2. *J Immunol* 2014;192(5):2280-2290.
16. Greenstein RJ, Su L, Shahidi A, Brown WD, Clifford A, Brown ST. Unanticipated *Mycobacterium tuberculosis* complex culture inhibition by immune modulators, immune suppressants, a growth enhancer, and vitamins A and D: Clinical implications. *Int J Infect Dis* 2014;26:37-43.
17. Young MRI, Day TA. Immune regulatory activity of vitamin D3 in head and neck cancer. *Cancers* 2013;5(3):1072-1085.

18. Chen Q, Mosovsky KL, Ross AC. Retinoic acid and α-galactosylceramide regulate the expression of costimulatory receptors and transcription factors responsible for B cell activation and differentiation. *Immunobiology* 2013;218(12):1477-1487.
19. Sada-Ovalle I, Skold M, Tian T, Besra GS, Behar SM. Alpha-galactosylceramide as a therapeutic agent for pulmonary *Mycobacterium tuberculosis* infection. *Am J Respir Crit Care Med* 2010;182(6):841-847.
20. Lee JM, Seo JH, Kim YJ, Kim YS, Ko HJ, Kang CY. The restoration of myeloid-derived suppressor cells as functional antigen-presenting cells by NKT cell help and all-trans-retinoic acid treatment. *Int J Cancer* 2012;131(3):741-751.
21. Jindani A, Dore CJ, Mitchison DA. Bactericidal and sterilizing activities of anti-tuberculosis drugs during the first 14 days. *Am J Respir Crit Care Med* 2003;167(10):1348-1354.
22. Wallis RS, Kim P, Cole S, Hanna D, Andrade BB, Maeurer M, Schito M, Zumla A. Tuberculosis biomarkers discovery: Developments, needs, and challenges. *The Lancet infectious diseases* 2013;13(4):362-372.
23. de Steenwinkel JE, Aarnoutse RE, de Knegt GJ, ten Kate MT, Teulen M, Verbrugh HA, Boeree MJ, van Soolingen D, Bakker-Woudenberg IA. Optimization of the rifampin dosage to improve the therapeutic efficacy in tuberculosis treatment using a murine model. *Am J Respir Crit Care Med* 2013;187(10):1127-1134.
24. de Steenwinkel JE, de Knegt GJ, ten Kate MT, Verbrugh HA, Hernandez-Pando R, Leenen PJ, Bakker-Woudenberg IA. Relapse of tuberculosis versus primary tuberculosis; course, pathogenesis and therapy in mice. *Tuberculosis (Edinb)* 2013;93(2):213-221.
25. De Steenwinkel JE, De Knegt GJ, Ten Kate MT, Van Belkum A, Verbrugh HA, Hernandez-Pando R, Van Soolingen D, Bakker-Woudenberg IA. Immunological parameters to define infection progression and therapy response in a well-defined tuberculosis model in mice. *Int J Immunopathol Pharmacol* 2009;22(3):723-734.
26. Swami S, Krishnan AV, Wang JY, Jensen K, Horst R, Albertelli MA, Feldman D. Dietary vitamin D(3) and 1,25-dihydroxyvitamin D(3) (calcitriol) exhibit equivalent anticancer activity in mouse xenograft models of breast and prostate cancer. *Endocrinology* 2012;153(6):2576-2587.
27. Giaccone G, Punt CJ, Ando Y, Ruijter R, Nishi N, Peters M, von Blomberg BM, Scheper RJ, van der Vliet HJ, van den Eertwegh AJ, et al. A phase I study of the natural killer T-cell ligand alpha-galactosylceramide (krn7000) in patients with solid tumors. *Clin Cancer Res* 2002;8(12):3702-3709.
28. Huizinga R, Easton AS, Donachie AM, Guthrie J, van Rijs W, Heikema A, Boon L, Samsom JN, Jacobs BC, Willison HJ, et al. Sialylation of *campylobacter jejuni* lipo-oligosaccharides: Impact on phagocytosis and cytokine production in mice. *PLoS One* 2012;7(3):e34416.
29. Schäffer MW, Roy SS, Mukherjee S, Ong DE, Das SK. Uptake of all-trans retinoic acid–containing aerosol by inhalation to lungs in a guinea pig model system—a pilot study. *Experimental lung research* 2010;36(10):593-601.
30. Mayer-Barber KD, Andrade BB, Barber DL, Hieny S, Feng CG, Caspar P, Oland S, Gordon S, Sher A. Innate and adaptive interferons suppress IL-1α and IL-1β production by distinct pulmonary myeloid subsets during mycobacterium tuberculosis infection. *Immunity* 2011;35(6):1023-1034.
31. Dutta NK, Bruiners N, Pinn ML, Zimmerman MD, Prideaux B, Dartois V, Gennaro ML, Karakousis PC. Statin adjunctive therapy shortens the duration of TB treatment in mice. *J Antimicrob Chemother* 2016;71(6):1570-1577.
32. Ahmad Z, Tyagi S, Minkowski A, Peloquin CA, Grosset JH, Nuermberger EL. Contribution of moxifloxacin or levofloxacin in second-line regimens with or without continuation of pyrazinamide in murine tuberculosis. *Am J Respir Crit Care Med* 2013;188(1):97-102.

33. Rohini K, Bhat S, Srikumar PS, Mahesh Kumar A. Assessment of serum calcium and phosphorus in pulmonary tuberculosis patients before, during and after chemotherapy. *Indian J Clin Biochem* 2014;29(3):377-381.
34. Lesokhin AM, Hohl TM, Kitano S, Cortez C, Hirschhorn-Cymerman D, Avogadri F, Rizzuto GA, Lazarus JJ, Pamer EG, Houghton AN, et al. Monocytic CCR2^{+} myeloid-derived suppressor cells promote immune escape by limiting activated CD8 T-cell infiltration into the tumor microenvironment. *Cancer Res* 2012;72(4):876-886.
35. Dorhoi A, Kaufmann SH. Tumor Necrosis Factor alpha in mycobacterial infection. *Semin Immunol* 2014;26(3):203-209.
36. Carpenter S, Ricci EP, Mercier BC, Moore MJ, Fitzgerald KA. Post-transcriptional regulation of gene expression in innate immunity. *Nat Rev Immunol* 2014;14(6):361-376.
37. Rajaram MV, Ni B, Morris JD, Brooks MN, Carlson TK, Bakthavachalu B, Schoenberg DR, Torrelles JB, Schlesinger LS. *Mycobacterium tuberculosis* lipomannan blocks TNF biosynthesis by regulating macrophage MAPK-activated protein kinase 2 (mk2) and microRNA mir-125b. *Proc Natl Acad Sci U S A* 2011;108(42):17408-17413.
38. Skerry C, Harper J, Klunk M, Bishai WR, Jain SK. Adjunctive TNF inhibition with standard treatment enhances bacterial clearance in a murine model of necrotic TB granulomas. *PLoS One* 2012;7(6):e39680.